



## REVIEW ARTICLE

# Cerebral cavernous malformations: Typical and atypical imaging characteristics

Danila Kuroedov<sup>1,2</sup> | Bruno Cunha<sup>1,2</sup>  | Jaime Pamplona<sup>1,2</sup> | Mauricio Castillo<sup>3</sup> | Joana Ramalho<sup>1,2</sup> 

<sup>1</sup>Department of Neuroradiology, Centro Hospitalar Universitário de Lisboa Central, Lisbon, Portugal

<sup>2</sup>NOVA Medical School, Universidade Nova de Lisboa, Lisbon, Portugal

<sup>3</sup>Department of Radiology, University of North Carolina School of Medicine, Chapel Hill, North Carolina, USA

## Correspondence

Joana Ramalho, Department of Neuroradiology, Centro Hospitalar Universitário de Lisboa Central, R. José António Serrano, 1150-199 Lisboa, Portugal. Email: [Joana-ramalho@netcabo.pt](mailto:Joana-ramalho@netcabo.pt)

## Funding Information

No funds, grants, or other support was received.

## Abstract

Cavernous malformations (CMs) are benign vascular malformations that maybe seen anywhere in the central nervous system. They are dynamic lesions, growing or shrinking over time and only rarely remaining stable. Size varies from a few millimeters to a few centimeters. CMs can be sporadic or familial, and while most of them are congenital, de novo and acquired lesions may also be seen. Etiology is still unknown. A genetic molecular mechanism has been proposed since a cerebral cavernous malformation gene loss of function was found in both familial and sporadic lesions. Additionally, recent studies suggest that formation of CMs in humans may be associated with a distinctive bacterial gut composition (microbioma). Imaging is fairly typical but may vary according to age, location, and etiology. Follow-up is not well established because CMs patients have a highly unpredictable clinical course. Angiogenic and inflammatory mechanisms have been implicated in disease activity, as well as lesional hyperpermeability and iron deposition. Imaging and serum biomarkers of these mechanisms are under current investigation. Treatment options, including surgery or radiosurgery, are not well defined and are dependent upon multiple factors, including clinical presentation, lesion location, number of hemorrhagic events, and medical comorbidities. Our purpose is to review the imaging features of CMs based on their size, location, and etiology, as well as their differential diagnosis and best imaging approach. New insights in etiology will be briefly considered. Follow-up strategies, including serum and imaging biomarkers, and treatment options will also be discussed.

## KEYWORDS

biomarkers, cavernous malformation, microbiome, MRI

## INTRODUCTION

Cavernous malformations (CMs) often simply designated as “cavernomas” or “cavernous angiomas” are angiographically occult vascular malformations without arteriovenous shunts. They are composed of thin-walled, dilated capillary spaces filled with blood at different stages of evolution with no intervening brain tissue.<sup>1</sup> The term “cavernous hemangiomas” should be avoided since hemangiomas are true pro-

liferating neoplasms classified (World Health Organization 2016) as nonmeningothelial mesenchymal tumors, while CMs are not.

CMs appear as single sporadic lesions or as multiple familial lesions. Although once thought of as a developmental disorder, the de novo appearance of CMs has been firmly established, most notably after radiation therapy.<sup>2</sup>

CMs are dynamic lesions, growing or shrinking over time and only rarely remaining stable. They vary in size, from millimetric to

This is an open access article under the terms of the [Creative Commons Attribution-NonCommercial-NoDerivs](https://creativecommons.org/licenses/by-nc-nd/4.0/) License, which permits use and distribution in any medium, provided the original work is properly cited, the use is non-commercial and no modifications or adaptations are made.

© 2022 The Authors. *Journal of Neuroimaging* published by Wiley Periodicals LLC on behalf of American Society of Neuroimaging.



giant lesions. Their growth mechanism has been hypothesized to be a result of repeated microhemorrhages and/or recanalization after intraluminal thrombosis.<sup>2</sup>

Although the majority of lesions are supratentorial (80-92%), they can be found throughout the entire central nervous system (CNS), including the infratentorial compartment (15%) and the spinal cord (5%).<sup>3</sup> Supratentorial CMs are more often seen in the deep white matter and cortico-subcortical frontal and temporal regions, while infratentorial lesions are more frequently seen in the pons and cerebellar hemispheres. Extra-axial lesions such as intraventricular, dural-based, cranial nerves (CN), cavernous sinus/pituitary fossa, and orbital CMs may also be seen.<sup>2,4</sup>

Imaging findings vary according to (1) pathology contents, including blood, thrombosis, and calcification; (2) locations, such as brain, spine, or extra-axial lesions; (3) size; and (4) clinical presentation, namely, incidental asymptomatic lesions or acute hemorrhagic symptomatic lesions. Despite the benign natural history of CMs, hemorrhage and/or mass effect in specific locations may be associated with significant morbidity or mortality if intracranial hemorrhage occurs, particularly in lesions located in the brainstem.<sup>5</sup>

Follow-up and treatment are not well defined and are dependent upon multiple factors, including clinical presentation, lesion location, number of hemorrhagic events, and medical comorbidities. Total surgical resection is the best treatment for patients with symptomatic lesions associated with recurrent hemorrhage, intractable epilepsy, and progressive neurological deficits, unless the location is associated with unacceptably high surgical risk.<sup>6-8</sup> Stereotactic radiosurgery has been used to treat CMs in deep-seated critical locations with some success.<sup>9</sup>

Our purpose is to review the imaging features of CMs based on their size, location, and etiology, as well as their differential diagnosis and best imaging approach. New insights in etiology will be briefly considered. Follow-up strategies, including serum and imaging biomarkers, and treatment options will also be discussed.

## EPIDEMIOLOGY

CMs are the second most common vascular malformation of the CNS after developmental venous anomalies (DVA).<sup>10</sup> They have an estimated incidence of 0.5%-1% in the general population<sup>11</sup> and constitute 10%-20% of all cerebral vascular malformations.<sup>12</sup>

Most CMs are incidental findings. Of the symptomatic CMs, 20%-30% occur between the third and fifth decade.<sup>13</sup> An autopsy study revealed that 90% of patients with CMs never had symptoms.<sup>14</sup> Prevalence of CMs is equal in males and females; however, women present more frequently with hemorrhage leading to symptoms.<sup>15</sup> CMs are less frequently reported in children.<sup>16</sup> Nevertheless, most of giant CMs occur in children.<sup>15</sup>

## ETIOLOGY

CMs may be sporadic or familial. Sporadic forms comprise a solitary CM with or without associated DVA or a cluster of lesions associated

with a DVA. Conversely, hereditary or familial forms—familial cerebral cavernous malformation syndrome (FCCM)—have multiple CMs, a family history of CMs in a first-degree blood relative, or a mutation genotyped at a cerebral cavernous malformation (CCM) gene locus. Mutations were found in three protein-encoding genes—CCM1 (KRIT 1), CCM2 (Malcavernin/MGC4607), and CCM3 (PDCD10)—that encode components of a single, heterotrimeric, adaptor protein complex.<sup>9,13</sup>

FCCM has been shown to be caused by heterozygous loss of function (LOF) mutations in one of these three genes and follow an autosomal dominant inheritance pattern. However, CMs present as focal lesions rather than a systemic vascular defect as might be expected if CMs were the result of haploinsufficiency. In fact, familial lesions have been shown to harbor biallelic mutations in endothelial cells lining the pathological vascular channels, while all cells in the body are heterozygous for the inherited gene. This means that loss of the normal allele via somatic mutation is required before lesion formation.<sup>17,18</sup>

Sporadic lesions, despite lacking inherited germline mutations, harbor somatic mutations of the same three CCM genes. This suggests an identical molecular mechanism related to CCM gene LOF in both familial and sporadic lesions.<sup>17,18</sup>

This two-hit theory indicates that the pathogenesis of CMs begins with an inherited (familial) or somatic (sporadic) mutation, followed by somatic mutations, which result in lesion genesis and growth.

Multiple CMs may also be acquired after radiation therapy. The multiplicity of lesions is related to radiation dose and (younger) age at radiation. Ionizing radiation has long been recognized as a potent source of DNA damage leading to genomic instability, supporting the key role for somatic mutations in CM pathogenesis.<sup>18</sup>

Lately, formation of CMs in humans has been associated with a distinctive bacterial gut composition (microbioma). Recent studies showed that CCM1- or CCM2-deficient mice with specific microbiomes may be prone to formation of CMs, while those with different microbiomes are not. A critical difference is the role of gram-negative bacteria (GNB) that produce a lipopolysaccharide (LPS) that acts on cell walls through the Toll-like receptor 4 (TLR4).<sup>19</sup> Tang et al. showed that activation of TLR4 by gram negatives or LPS accelerates CM formation, while genetic or pharmacologic blockade of TLR4 signaling prevents CMs formation in mice.<sup>19</sup>

Another article on a large cohort of human subjects with and without CMs assessed the particularities of their gut microbiome. The authors demonstrated that patients with CCMs have distinctive microbiomes compared to healthy individuals. Analysis at the biosynthesis and gene levels indicated that LPS synthesis-related genes are more abundant in CCM patients, consistent with the role of gut-generated LPS driving CMs formation.<sup>20</sup>

The familial form of CCM3 develops malformations decades earlier than those with CCM1 or CCM2 mutations and are more likely to suffer disabling brain hemorrhage and stroke.

A study by Tang et al. partly undertaken in mice showed that the effect of absent CCM3 in the blood capillary cells in mice was similar to that caused by the absence of CCM1 and CCM2.<sup>21</sup> Comparing the microbiome in humans, by analyzing fecal samples, the authors

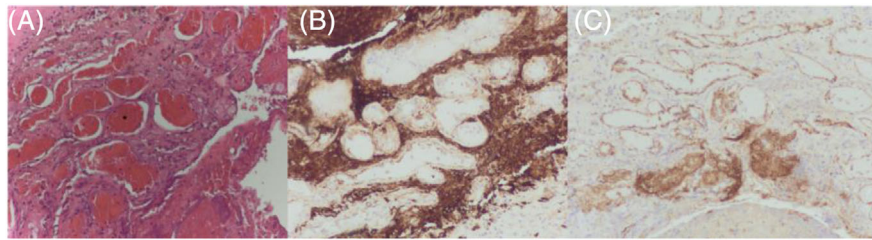


**FIGURE 1** (Courtesy of Dr. Carlos Pontinha) Cavernous malformations histopathology. Hematoxylin and eosin-stained section (A) showing blood-filled cavity (\*) surrounded by thick and thin endothelium-lined vascular channels CD31 positive (B) with adjacent gliotic cerebral parenchyma glial fibrillary acidic protein positive (C). Hemosiderin-laden macrophage may also be seen

also found a significant difference between the microbiomes of those with familial CCM3 and those without it. However, the microbiomes of those with CCM3 were indistinguishable from those with CCM1 and CCM2, thus the more aggressive nature of CCM3 cannot be attributed to only the microbiome. The article also showed that abnormal CCM3 in mice was found to reduce mucus formation. PDCD10 is required for the secretion of mucus by goblet cells. This function is not shared with KRIT1 and CCM2. Mucus forms a barrier in the gut lining that helps prevent billions of bacteria from crossing into the bloodstream. Further, these authors showed that other mechanisms that reduce the mucus lining also caused an increase in CM formation.

The overall conclusion is that formation of CMs in humans is associated with a distinctive bacterial gut composition and mucus production. These unexpected gut-brain disease axes suggest that future diagnostic and therapeutic strategies based on manipulation of the gut microbiome could be used to treat FCCM disease.

## HISTOPATHOLOGY

Despite the genotype, CMs are all histologically identical, characterized by abnormal dilated vascular spaces (endothelial-lined caverns) with no intervening neural tissues. Electron microscopy and immunohistochemistry identify specific differences between the architecture of normal cerebral blood vessels and those found in CMs. In contrast to the normal cerebral vessels, the vascular walls of CMs show endothelial cell fenestrations, large endothelial cell junction gaps, absence of basal lamina, lack of astrocytic foot process, and rare pericytes (Figure 1). These ultrastructural characteristics create a dysfunctional blood-brain barrier, which permits the chronic extravasation of red blood cells through the vessel walls and results in microhemorrhages and hemosiderin deposition in the surrounding parenchyma.<sup>22</sup>

## SYMPTOMS

Symptoms vary according to lesion location and are usually associated with hemorrhage and/or mass effect. Seizures are the most common clinical presentation.<sup>1</sup>

The annual risk of hemorrhage varies widely (1%-6.8%).<sup>23-25</sup> The most significant predictor of hemorrhage is previous hemorrhage.<sup>26</sup>

Other factors associated with higher risk of hemorrhage include early age of lesion onset, female gender, large CM, multiplicity, brain stem location, and accompanying DVA.<sup>27</sup> Hormones influence the behavior of the CM. Women may have acute clinical symptoms and aggravation of already existing CMs during the first trimester of pregnancies.<sup>28-31</sup>

## IMAGING FINDINGS

### Computed tomography

On CT, CMs usually appear as focal areas of increased density in the brain often without mass effect (Figure 2). Increased density represents calcium, blood, or a combination of them. Usually, no enhancement is seen after contrast administration. CMs are more conspicuous when a recent hemorrhage occurs, and they may be surrounded by vasogenic edema (Figure 3). A total of 30%-50% of cavernomas are not detectable by CT. The differential diagnosis on CT includes low-grade calcified neoplasms, hemorrhage (of other causes), calcified infectious sequel, and other vascular malformations.<sup>32</sup>

### Magnetic resonance imaging

MRI is the gold standard for imaging CMs. The MRI protocol should include conventional T1- and T2-weighted imaging (WI), axial gradient recalled echo (GRE)/susceptibility-weighted imaging (SWI), and diffusion-weighted imaging (DWI).

In the classic MRI “popcorn” appearance, CMs are seen as well-circumscribed lobulated lesions with a reticulated core of heterogeneous signal intensity (SI) on both T1 and T2-WI, resulting from thrombosis, fibrosis, calcification, and hemorrhage (Figure 4). Extracellular and intracellular methemoglobin and thrombosis are responsible for the high T1 signal within the lesion, while calcifications, fibrosis, and acute and subacute blood are responsible for the low signal areas. Blooming in GRE/SWI sequences is characteristic, corresponding to hemosiderin and iron deposition in the surrounding brain parenchyma.<sup>32</sup> The DWI sequences usually show mixed signal (Figure 5).

Based on MRI, Zabramski et al. classified CMs into four types: Type I are homogeneously hyperintense on T1-WI, representing subacute

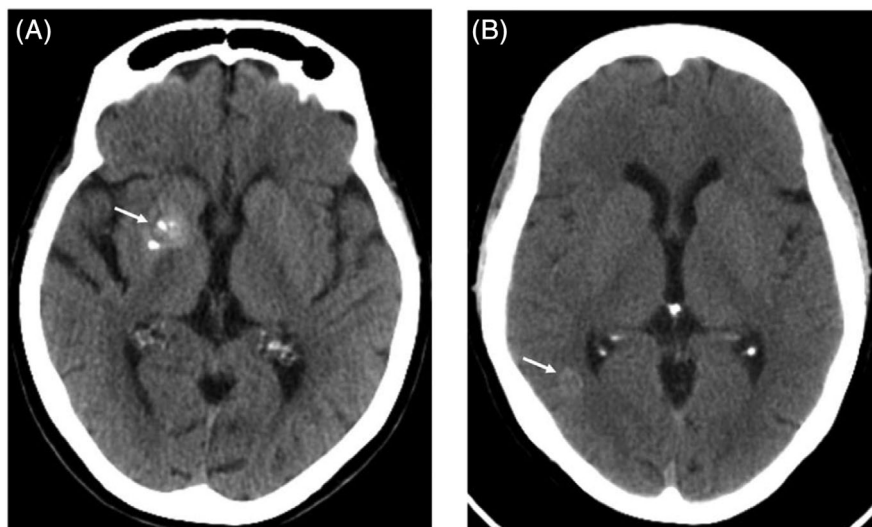


**FIGURE 2** Typical appearance of cerebral cavernomas on CT. Axial reconstructions of brain CT. Focal nodular areas of increased density (arrows) in the right lentiform nucleus (A) and right temporal lobe (B). Note the associated calcified components in the lentiform cavernoma

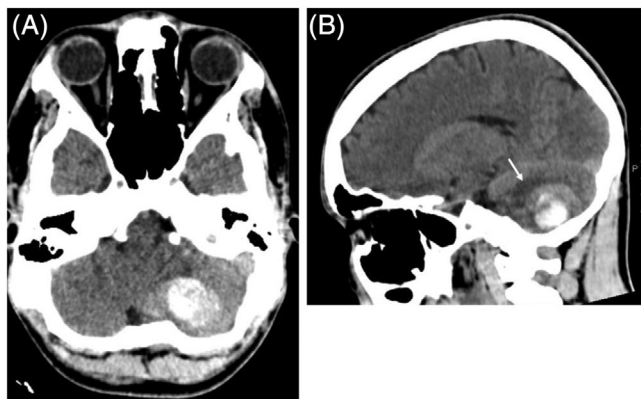


**FIGURE 3** CT images of cerebellar cavernoma with recent hemorrhage. Axial (A) and sagittal (B) reconstructions of brain CT. Hyperdense cerebellar hematoma with associated perilesional edema (arrow in B) and effacement of the adjacent sulci. This was a cerebellar cavernoma with recent bleeding

hemorrhage dominated by methemoglobin<sup>33</sup>; Type II are most common (50-67%) and show the classic “popcorn” appearance as described above (heterogeneous lesions on T1 and T2-WI); Type III are isointense to hypointense on both T1 and T2-WI, representing a predominance of chronic blood products; and type IV are seen as tiny, often multiple, punctate foci with low T1 and T2 SI, best seen on GRE or SWI sequences<sup>3</sup> (Table 1).

Atypical CMs may show variable contrast enhancement, prominent perilesional vasogenic edema, mass effect, and cystic components and have appearances similar to brain tumors. The clinical and prognostic significance of these findings is not clear (Figure 6).

After acute hemorrhage, a parenchymal hematoma may be the only imaging manifestation of a CM (Figure 7). Yun et al. reported a T1 hyperintensity in the perilesional edema surrounding an acute or subacute hematoma in 62% of CMs with recent hemorrhage.<sup>22</sup> This finding

was highly specific (98%) and predictive (95%) for CM. This sign helps differentiate hemorrhagic CMs from other hemorrhagic lesions, such as tumors or other vascular malformations (Figure 8).

The combination of CM and DVA should be considered since both disorders coexist in about 30% of patients.<sup>34</sup> DVAs appear as linear enhancing structures or caput-medusae (radial orientation of small vessels draining to a common larger collector vein that resemble the hair of Medusa) in combination with lesions typical of CMs (Figure 9). They should be reported as such since venous infarcts have been reported after surgery due to inadvertent resection of the DVA.

Vascular hyperpermeability and chronic iron deposition are cardinal features of CMs. Dynamic contrast-enhanced quantitative perfusion (DCEQP) and quantitative susceptibility mapping (QSM) have been used in research studies to quantitatively measure CMs permeability and iron content, respectively.<sup>35</sup> Other advanced imaging techniques, such as diffusion tensor imaging (DTI) and task-based functional MRI, have a role in surgical planning/navigation.

### Digital subtraction angiography

DSA has no role in brain CMs evaluation since these lesions are angiographically occult. It may be performed for “atypical” lesions to exclude other vascular malformations or concurrent vascular anomalies<sup>1,2</sup> (Figures 10 and 11).

### FOLLOW-UP AND BIOMARKERS

The natural history of CMs is unpredictable. There are no data or guidelines to guide follow-up in asymptomatic patients. In these patients, serial imaging remains controversial. Conversely, new neurological symptoms suggestive of hemorrhage warrant repeat imaging, which should be performed as soon as possible. Imaging follow-up is also

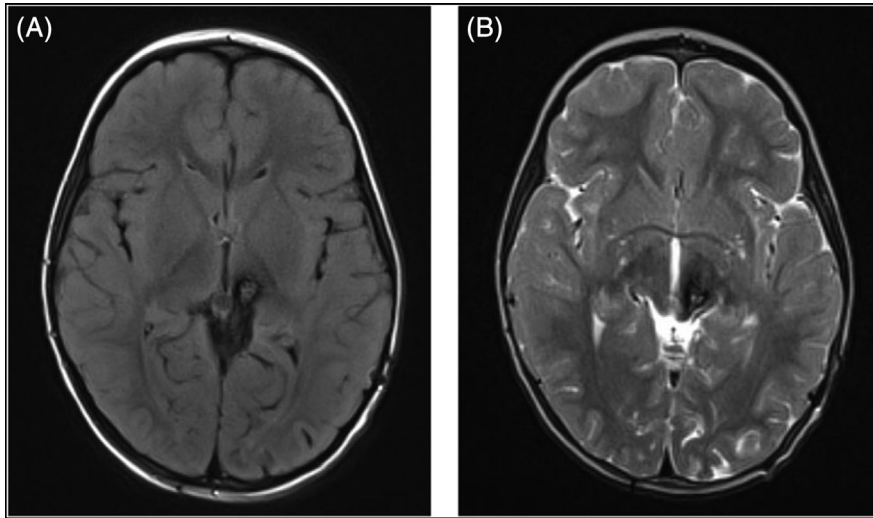


**FIGURE 4** Thalamic cavernoma. Axial T2 fluid-attenuated inversion recovery (FLAIR) (A) and T2-weighted imaging (B). Left thalamic lesion with heterogeneous signal intensity and a peripheral T2/FLAIR hypointense ring—this is the characteristic “popcorn-like” appearance of a cavernoma

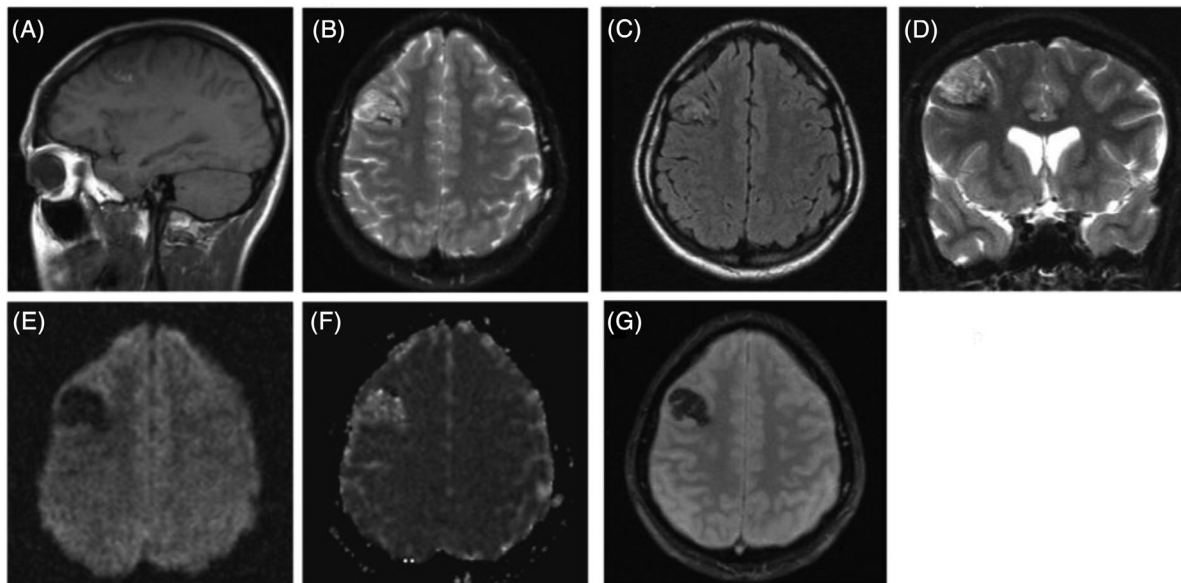


**FIGURE 5** Right middle frontal gyrus cavernoma. Sagittal T1-weighted imaging (WI) (A), axial T2-WI (B), T2 fluid-attenuated inversion recovery (C), coronal T2-WI (D), axial diffusion-weighted imaging (DWI) (E), apparent diffusion coefficient (ADC) map (F), and axial gradient recalled echo (G). Intraparenchymal expansile lesion in the right middle frontal gyrus with heterogeneous signal intensity on T1-WI and T2-WI (“popcorn” appearance), with facilitated heterogeneous diffusion on DWI/ADC and blooming effect on T2\*

**TABLE 1** CMs classification according to Zabramski<sup>33</sup>

Lesion type	MRI findings	Histopathology
Type 1	Homogeneously hyperintense on T1-WI	Subacute bleed dominated by methemoglobin
Type 2	Classic “popcorn” appearance, heterogeneous lesions on T1 and T2-WI	Lesions with loculated hemorrhage and thromboses of varying ages enveloped by gliotic tissue, hemosiderin rim
Type 3	Isointense to hypointense on both T1 and T2-WI	Chronic blood products, hemosiderin rim
Type 4	Tiny, often multiple, punctate foci with low T1 and T2 signal, best seen on GRE or SWI sequences	Multiple punctate microhemorrhages

Abbreviations: GRE, gradient recalled echo; SWI, susceptibility-weighted imaging; WI, weighted imaging.

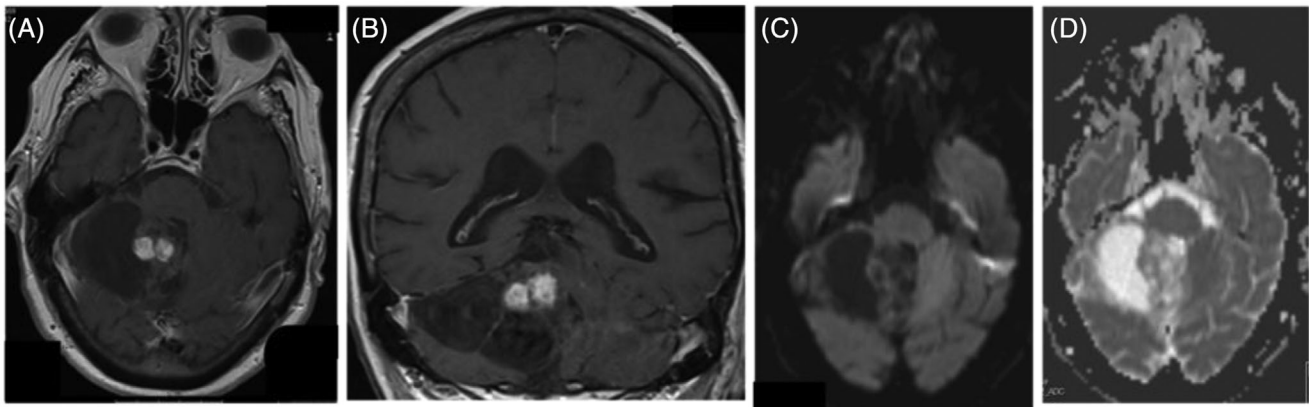


**FIGURE 6** Cerebellar cavernoma. Axial (A) and coronal (B) contrast-enhanced T1-weighted imaging axial diffusion-weighted imaging (C) and apparent diffusion coefficient map (D). Large right cerebellar hemisphere intraaxial cystic mass with two solid contrast-enhancing mural nodules (which do not show restricted diffusion). This is a posterior fossa pseudo-tumoral appearing cavernoma (histologically proven) that could easily mimic a cystic tumor such as a pilocytic astrocytoma or a hemangioblastoma

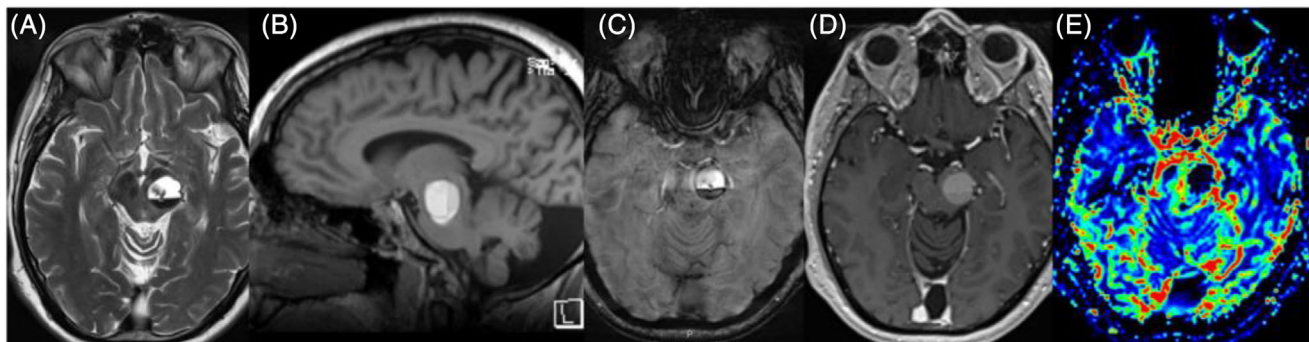


**FIGURE 7** Companion case of a thalamic cavernoma with recent hemorrhage. Axial T2-weighted imaging (WI) (A), sagittal T1-WI (B), axial gradient recalled echo (C), contrast-enhanced T1-WI (D), and cerebral blood flow map of dynamic susceptibility contrast MR perfusion (E). Left thalamic expansive with a fluid level (T2 hyperintense signal anteriorly and T2 hypointense signal with a hypointense rim on T2\* posteriorly) and hyperintense signal on T1-WI, with no contrast enhancement and showing marked hypoperfusion. This is a subacute hematoma with an underlying cavernoma

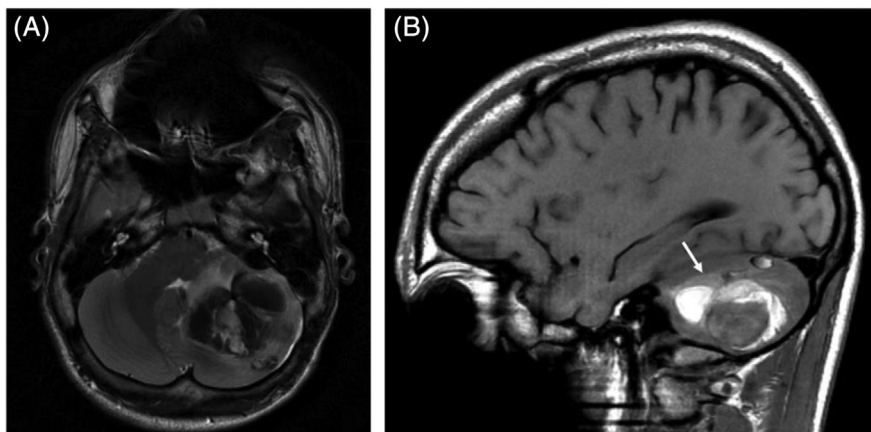


**FIGURE 8** MRI of cerebellar cavernoma with recent hemorrhage. Axial T2-weighted imaging (WI) (A) and sagittal T1-WI (B). Left cerebellar hemisphere acute and subacute hematoma (same case as Figure 3). Note the T1 hyperintensity of the perilesional edema (arrow). This finding is highly suggestive of a cavernoma as the cause of the hematoma

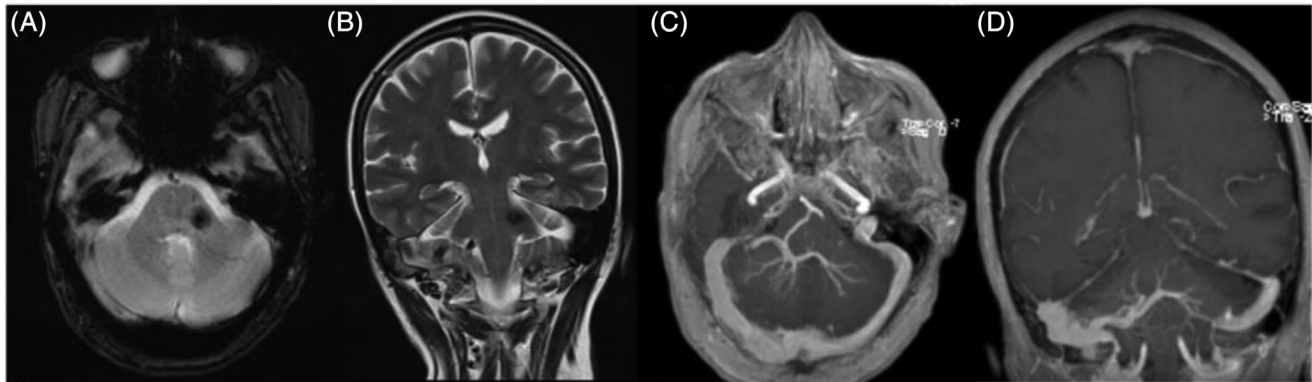


**FIGURE 9** Cavernous hemangioma with an associated developmental venous anomaly (DVA). Axial susceptibility-weighted imaging (A), coronal T2-weighted imaging (B), and axial (C) and coronal (D) maximum-intensity projection reformations of MR venography. Left middle cerebellar peduncle cavernoma with an associated DVA, showing the typical caput medusae sign of draining veins into the venous collector, which later drains to the left transverse sinus

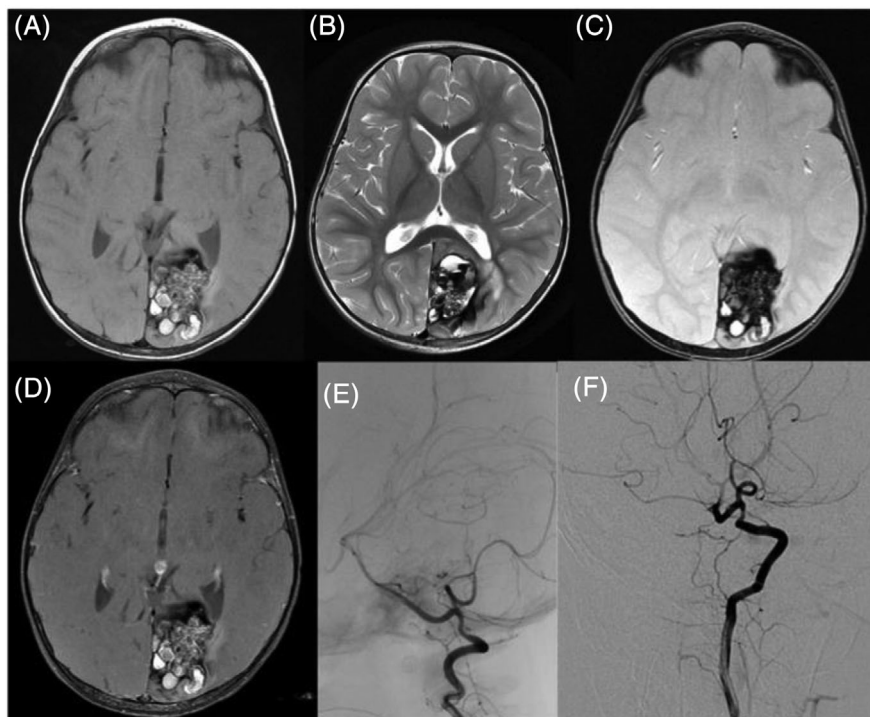


**FIGURE 10** Cortico-subcortical cavernoma. Axial T1-weighted imaging (WI) (A), T2-WI (B), gradient recalled echo (C), and contrast-enhanced T1-WI (D). Lateral view of right vertebral artery injection (E) and lateral view of left internal carotid artery injection (F) during digital subtraction angiography (DSA). Heterogenous left cortico-subcortical occipital parenchymal lesion that could represent an arteriovenous malformation. It shows several T1 hyperintense components compatible with recent bleeding, T2 hyper and hypointense regions, a T2 hypointense perilesional rim, and blooming effect on T2\*. DSA images did not identify any abnormal vascular structures. This is a surgically proven cavernoma

suggested whenever CMs are shown to have grown 5 mm or more or in patients with risk factors for CMs mimics (e.g., older age or history of systemic cancer).<sup>36</sup>

Recently, based on new discoveries implicating angiogenic and inflammatory mechanisms in disease activity, several blood biomarkers have been used for monitoring and predicting disease aggressiveness. These include plasma levels of calciferol (25-hydroxyvitamin D) and non-high-density lipoprotein cholesterol, inflammatory cytokines,

and angiogenic plasma parameters. Some of these peripheral plasma biomarkers reflect seizures and recent hemorrhage and others correlate with disease aggressiveness and predict future clinical activity.<sup>35,37-39</sup> Further work is needed to define the use of these biomarkers in clinical practice.

As stated before, DCEQP and QSM may also be used as biomarkers to monitor the course of the disease and effect of therapy, to evaluate lesion development and bleeding (as measured by iron deposition

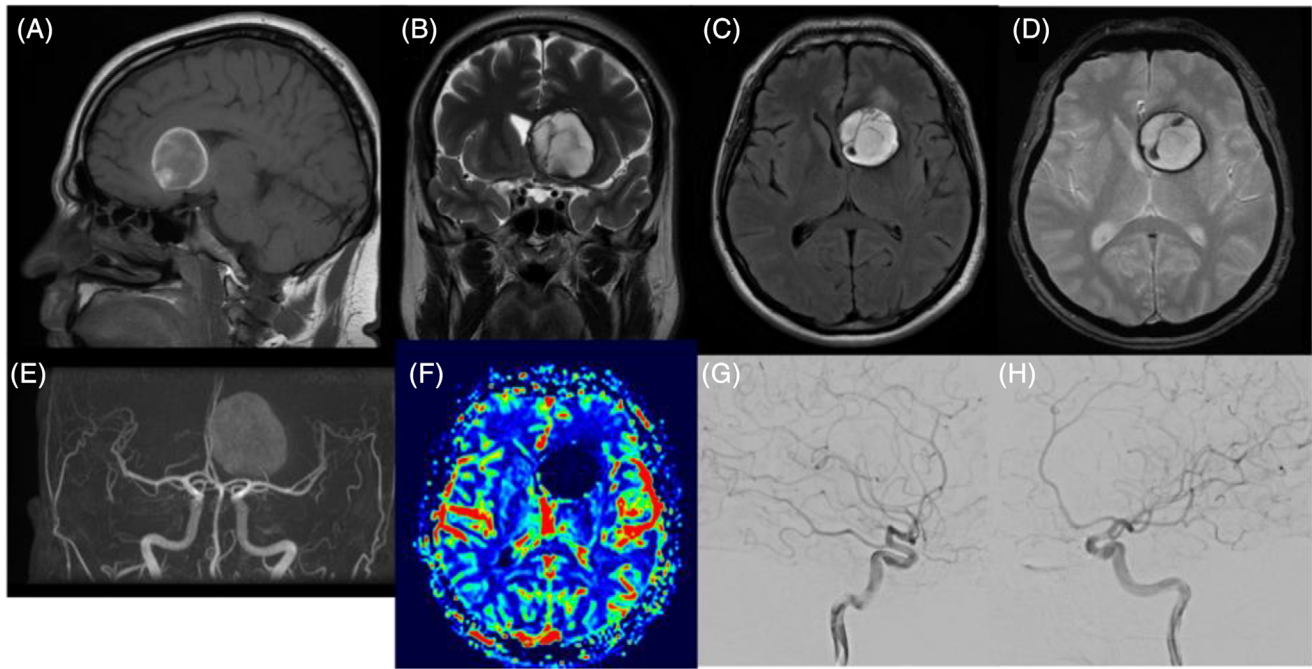


**FIGURE 11** Sagittal T1-weighted imaging (WI) (A), coronal T2-WI (B), axial fluid-attenuated inversion recovery (C), and gradient recalled echo (D). Three-dimensional reconstructions of time-of-flight MR angiography (E). Cerebral blood flow map of dynamic susceptibility contrast MR perfusion (F). Lateral (G) and anteroposterior (H) views of left internal carotid artery (ICA) injection during digital subtraction angiography (DSA). Left suprasellar space occupying lesion in close relationship to the left internal carotid artery appearing to represent a top of the ICA thrombosed aneurysm. This was not confirmed on DSA and following surgery proved to be a cavernoma

in QSM), and to assess the vascularity of CMs (as measured by DCEQP).<sup>35</sup>

## TREATMENT

Current treatment options for CMs include observation, microsurgical resection, and radiosurgery. Asymptomatic lesions, irrespective of location, should be treated conservatively with appropriate clinical and MRI follow-up. Clinical observation determines if a newly discovered lesion or increase in the size of a preexisting one is asymptomatic or whether a patient has experienced seizures or has new neurological deficits.

Microsurgical resection may be considered in patients with asymptomatic CMs in noneloquent areas to prevent future hemorrhage, when lifestyle, occupation, and the psychological burden outweigh the risk of surgical morbidity.<sup>40</sup> Surgical resection is indicated in patients with symptomatic CMs located in noneloquent areas who present with new neurologic deficits, recurrent hemorrhage, and medically refractory epilepsy.<sup>40</sup> An increase in lesion size should not be used as sole criterion for surgery. Intraoperative neuronavigation, DTI of adjacent fiber tracts, and electrophysiological monitoring assist in safe and total excision of lesions.

Brain stem CMs treatment is controversial since they have a higher risk of hemorrhage, which may be fatal, but they also have a higher risk of death from surgery complications.<sup>40-42</sup>

Radiosurgery plays an increasingly important role in deep-seated CMs and patients with high surgical risk over the past 20 years. Gamma Knife (GKS) decreases the risk of hemorrhage in patients presenting with symptomatic hemorrhagic lesions, including brainstem lesions, and allows for seizure control in some patients.<sup>43</sup>

Different medical treatments are currently under investigation. These treatments aim to stabilize blood vessels to reduce oozing and risk of hemorrhage, prevent re-hemorrhage, shrink lesions or cause them completely to resolve without surgery, prevent lesions from recurring after surgery, remove iron deposits in the brain and spinal cord left behind by hemorrhage, prevent systemic effects of familial CCM, and stop familial CCM from being passed to the next generation. Other determinations include how long to treat a patient, at what stage of the illness, and what therapeutic risk is justified and acceptable. Ongoing clinical trials include atorvastatin (RHO kinase inhibitor), superoxide dismutase, vitamin D3, propranolol (a beta blocker), and gut bacteria modification.

## FAMILIAL CAVERNOMATOSIS

FCCM is defined by presence of multiple CMs (more than five), occurrence of CMs in at least two members of a family, or presence of a mutation in one of the three CCM genes causing FCCM (Table 2). However, the presence of a single CM in an individual, even without a history of FCCM, does not exclude FCCM.<sup>44</sup>

**TABLE 2** FCCM genes<sup>36</sup>

Locus	Gene	Chromosome locus	Incidence	Clinical findings
Name	Directly interact in a heterotrimeric adaptor complex (CCM complex)			
CCM1	KRIT1	7q21.2	40%	
CCM2	CCM2	7p13	} 60%	CCM3—More severe disease course; Manifest at a younger age (frequently with intracranial hemorrhage). Close relation with cutaneous vascular malformations, spinal cord cavernomas, scoliosis, and benign central nervous system tumor including meningioma, astrocytoma, and vestibular schwannoma. <sup>36</sup>
CCM3	PDCD10	3q26.1		

FCCM is an inherited autosomal dominant trait with incomplete penetrance and variable expression.<sup>35,45</sup> The identity of the mutated gene has been associated with several clinical characteristics. CCM1 mutation is associated with cutaneous vascular lesions, while individuals with CCM2 mutations are more likely to be asymptomatic and have a lower number of lesions. CCM 3 mutations is related with more aggressive disease and its severity is attributable to the role of PDCD10 in the gut epithelium not shared with KRIT1 or CCM2, as discussed previously.

More than 350 distinct CCM1/CCM2/CCM3 mutations have been published to date. There are four known founder mutations in the CCM genes that account for substantial fraction of FCCM cases. The most common of these is a KRIT1 mutation present in most Hispanic American cases of FCCM.<sup>18</sup>

A total of 20%-50% of FCCM patients remain asymptomatic and lesions are incidentally discovered during head imaging.<sup>46</sup> Although FCCM has been reported in infancy and childhood, most patients present during the second to fifth decades of their lives. FCCMs most commonly present with seizures (38-55%) and focal neurological deficits (35%-50%).<sup>44</sup>

A recent study provides evidence that obesity may be a risk factor for CMs hemorrhage. Other previously reported risk factors including hypertension, diabetes, and hyperlipidemia and current nicotine abuse showed no such effects.<sup>47</sup>

Lesions may be located either supratentorial (75%) or infratentorial (20%) and even in the spinal cord (5%). In typical cases, brain MRI shows multiple bilateral and diffuse lesions of variable size with susceptibility-induced signal loss well seen on GRE sequences and even better seen on SWI (Figure 12). A degree of blooming seen as a hazy halo of signal loss around the lesions leads to overestimation of the actual size of the lesions.<sup>44</sup> A spine MRI at the time of diagnosis may be helpful to exclude cord CMs.

In the differential diagnosis, other causes of micro- and macrobleeds must be considered including cerebral amyloid angiopathy, (chronic) hypertensive encephalopathy, hemorrhagic metastases, and trauma (when in proper context). Neurocysticercosis, cerebral vasculi-

tis, and radiation-induced cavernous malformations should be ruled out.

Due to the dynamic nature of CMs, new lesions may appear at a rate of 0.2-0.4 lesions per patient year.<sup>48</sup> Some authors suggest a control brain MRI every 2 years (using GRE or SWI sequences) or whenever new neurologic symptoms occur.<sup>44</sup> Screening brain MRI examinations of family members is also suggested.<sup>44</sup>

Regarding treatment, patients with FCCM having small multiple lesions are managed conservatively. Surgical removal of lesions associated with symptoms, such as drug-resistant seizures or focal deficits, may be justified, even when other lesions are present.<sup>44</sup>

There may be an increased risk of hemorrhage with certain medications such as nonsteroidal anti-inflammatory drugs.<sup>41</sup> Additionally, the risk-benefit of medications that increase hemorrhage frequency (heparin and coumarin-type drugs) should be weighed carefully before they are used.<sup>44</sup>

## SPINAL CORD CAVERNOUS MALFORMATIONS

Intramedullary spinal cavernomas (ISCMs) are rare vascular lesions that account for 5%-12% of all spinal vascular lesions. ISCMs represent 3%-5% of CNS CMs.<sup>49</sup>

An ISCM may become clinically apparent following an acute intramedullary hemorrhage with mass effect, with acute onset of neurological deficits. On the other hand, worsening of preexisting symptoms may be the result of recurrent small hemorrhages. Repetitive intralesional microhemorrhages can lead to a slowly progressive decline in neurological function.

Imaging features of ISCMs are like those found in the intracranial compartment (Figure 13). However, in the acute hemorrhagic phase, it may be necessary to perform spinal angiography to rule out a small arteriovenous malformation (AVM). Additionally, postcontrast MRI demonstrates subtle or no contrast enhancement of ISCMs.<sup>49</sup>

Despite the morphological similarities between intracranial CMs and ISCMs, some authors favor microsurgery with intraoperative

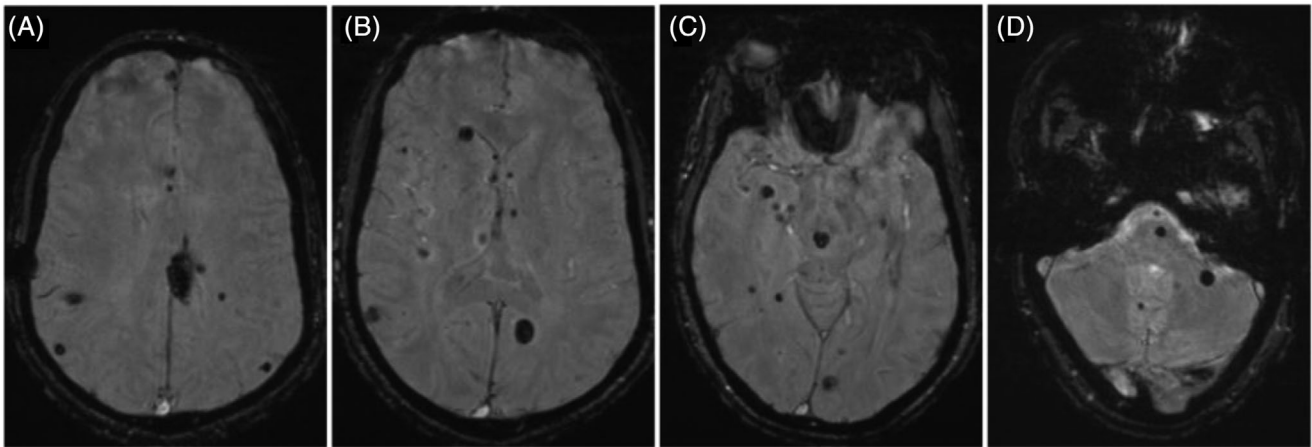


**FIGURE 12** Familial cavernomatosis. Axial susceptibility-weighted imaging, multiple slices. Multiple round hypointense lesions of different sizes. This is the blooming susceptibility phenomenon produced by hemosiderin deposits of multiple cavernous malformations in a patient with familial cavernomatosis

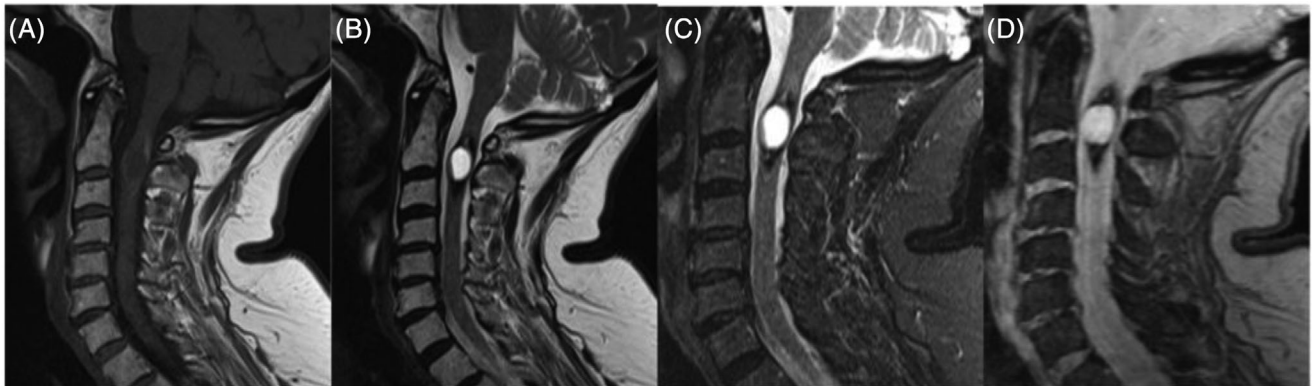


**FIGURE 13** Spinal cord cavernoma. Sagittal T1-weighted imaging (WI) (A), T2-WI (B), short tau inversion recovery (C), and gradient recalled echo (D). Cervical intramedullary cystic-like lesion with a T1 hyperintense and T2 hypointense rim

neurophysiologic monitorization over a “wait and see” protocol and other conservative treatments.<sup>50</sup>

## GIANT CAVERNOUS MALFORMATIONS

A giant cavernous malformation (GCM) is arbitrarily defined and varies according to different authors. Lawton et al. proposed the most accepted definition in 2004 that defines it as a lesion larger than 6 cm in at least one dimension.<sup>51</sup>

The cause of the development and growth of CMs is uncertain. A universally accepted theory for formation of GCMs growth consists of repeated hemorrhage that leads to clot formation and organization, pseudocapsule formation, and expansion of the lesion. Another explanation is that GCMs form and expand by the same mechanisms as chronic subdural hematomas, by endothelialization of small hematomas that they create.<sup>52</sup> Yet another hypothesis suggests that the growth of GCMs mimics that of a neoplasm where lesions are either induced to produce or spontaneously produce angiogenic fac-

tors that allow angiogenesis.<sup>15,31,53</sup> Engorgement and/or recruitment of adjacent feeding vessels, episodes of peri-lesional hemorrhages, and hormonal influences may also play a role in the growth of GCMs.<sup>15</sup>

Giant intracranial extra-axial CMs are reported in the scalp, pericranium, parietal convexity, pituitary gland, middle cranial fossa, and cavernous sinus.<sup>54–57</sup> Giant intracranial and intraaxial cerebral parenchymal CMs are extremely rare.<sup>58</sup> They are more common in children and young adults and no familial association has been reported. All cases described in the literature are supratentorial and solitary. The most common locations are the frontal or frontoparietal regions but they have also been reported in other locations, including the occipital and temporal lobes.<sup>59,60</sup>

GCMs are more likely to present with seizures and mass effect, causing progressive neurological deficits, and rarely present with overt hemorrhages. They can also be clinically occult if located in “silent” cortical areas, particularly the frontal lobes.<sup>61,62</sup>

On MRI, most of the GCMs present as heterogeneous and multicystic lesions related the blood of different ages with multiple complete hemosiderin rings resulting in a “bubbles of blood” appearance. Fluid

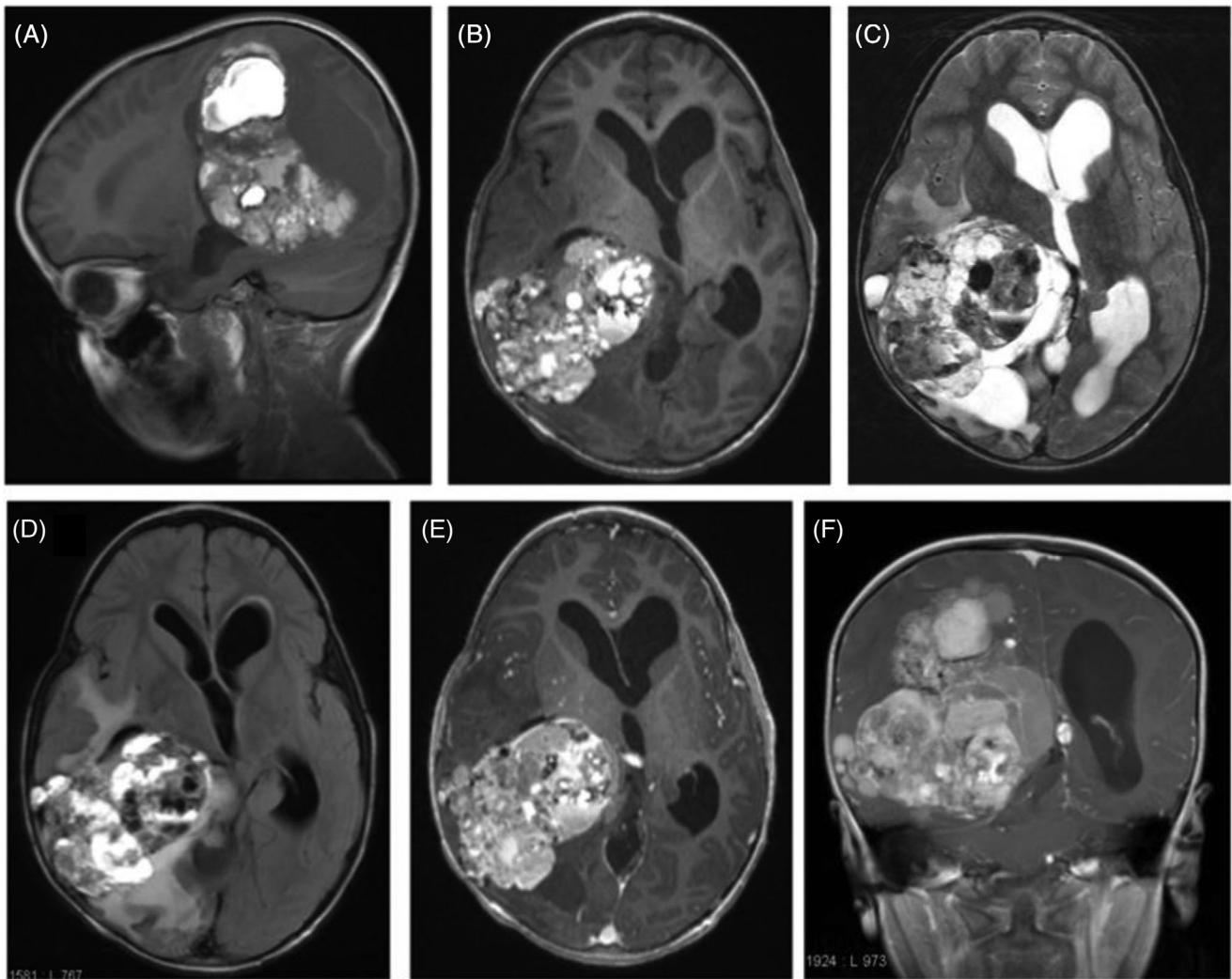


**FIGURE 14** Giant cavernoma. Sagittal (A) and axial (B) T1-weighted imaging (WI), axial T2-WI (C) and fluid-attenuated inversion recovery (D), and axial (E) and coronal (F) contrast-enhanced T1-WI. Large intraaxial extraventricular heterogeneous mass in the right temporo-occipitoparietal lobes with areas of cystic changes, hemorrhage, and calcifications (CT not shown). The solid components show avid contrast enhancement. There is surrounding edema and mass effect with midline shift and ventricular enlargement (obstructive hydrocephalus). This is a surgically proven giant cavernoma

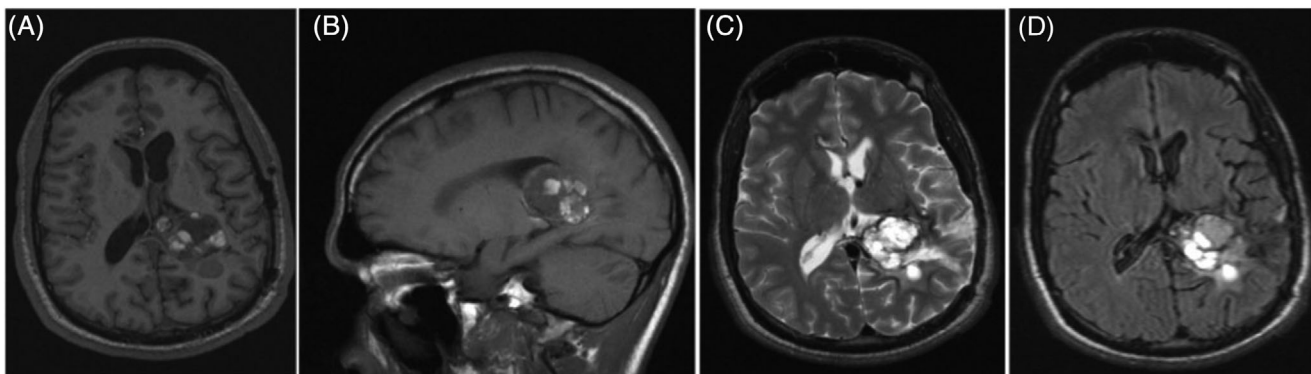


**FIGURE 15** Intraventricular cavernoma. Axial (A) and sagittal (B) T1-weighted imaging (WI) and axial T2-WI (C) and fluid-attenuated inversion recovery (D). Intraventricular heterogeneous multilobulated expansile lesion in the atrium of the left lateral ventricle with multiple T1 hyperintense areas and a T2 hypointense peripheral rim. There is some perilesional vasogenic edema in the adjacent parietal white matter. This intraventricular cavernoma with a pseudo-tumoral appearance could mimic an intraventricular tumor such as an ependymoma or intraventricular metastasis

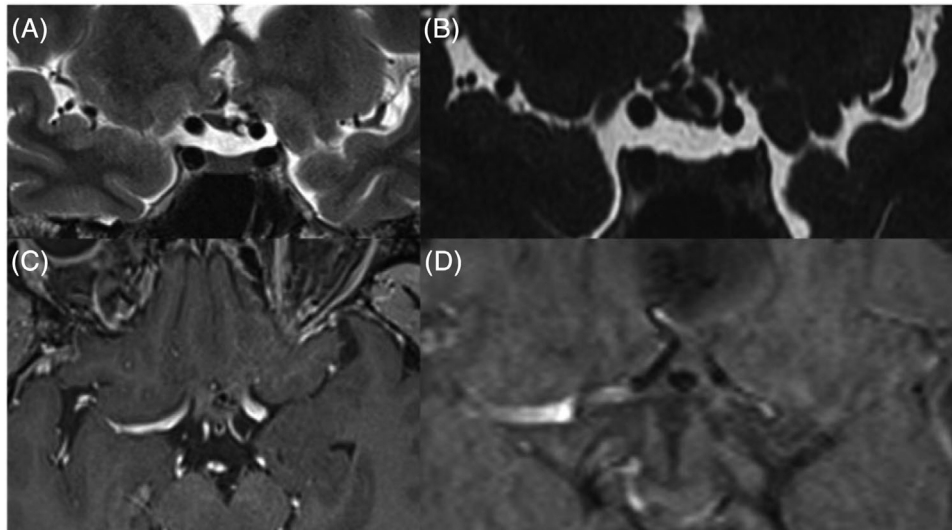


**FIGURE 16** Optic chiasm cavernous malformation. Coronal T2-weighted imaging (WI) (A) and T2-driven equilibrium radio frequency reset pulse (B) and axial contrast-enhanced fat-saturated T1-WI (C) and susceptibility-weighted imaging (SWI) (D). A surgically proven cavernous malformation located superiorly and adjacent to the left side of the optic chiasm, with local mass effect. A mild hypointense rim of hemosiderin can also be appreciated in SWI—"iron ring sign"

levels are common and minimal contrast enhancement is seen. DVAs may also be present and help reach the correct diagnosis (Figure 14). Extensive calcifications and dural invasion have been reported.<sup>15</sup>

Differential diagnosis includes hemorrhagic and calcified neoplasms, inflammatory/infectious masses or granulomas, subacute hematoma of other etiology, and thrombosed AVMs.<sup>62</sup> Differentiation between tumors and tumor-like lesions is essential for planning adequate treatment and estimating outcomes and prognosis.

Treatment involves evacuation of neighboring hematoma and, if possible, complete resection of the lesion, sparing any associated DVAs. The outcome is excellent with improvement in seizure control in most patients.<sup>62,63-65</sup> But in patients with intractable seizures, the outcome may be less favorable.<sup>62</sup> The role of radiosurgery and stereotactic radiotherapy for deep-seated surgically inaccessible GCM is controversial.<sup>66,67</sup>

## EXTRA-AXIAL LESIONS

Extra-axial CMs are rare and have the same histological features as intraaxial lesions but they have different clinical presentations, natural history, and imaging findings. They can be orbital, intraventricular, or dural based. Cranial nerves CMs may also be seen.

### Intraventricular cavernous malformations

Intraventricular CMs (IVCMs) represent about 2.5%-10.8% of all intracranial CMs.<sup>68,69</sup> The lateral ventricles are the most frequent location, followed by the third and fourth ventricles.<sup>70</sup> These lesions are usually voluminous. Lack of surrounding brain tissue allows unrestricted growth and their increased tendency for intralesional bleeding

may also contribute to their growth.<sup>71</sup> In the literature, the mean size of these lesions is reported to be 23-28 mm.<sup>66,70</sup>

The most common symptoms are due to mass effect, followed by hemorrhage and seizure. The presence of hydrocephalus depends on their location. Third ventricle lesions, particularly those located in the foramen of Monro, often present with hydrocephalus.

On CT, these lesions are moderately hyperdense with minimal contrast enhancement and most of them show calcifications.<sup>69</sup> MRI may show a central area of high T1 signal due to methemoglobin. Low T1 and T2 signal areas may be present due to calcifications and fibrosis. The hemosiderin paramagnetic effect causes a peripheral rim of a low signal. Contrast enhancement is variable (Figure 15).

The radiological differential diagnosis of IVCMs includes intraventricular tumors, such as choroid plexus papilloma, ependymoma, central neurocytoma, intraventricular meningioma, and subependymal giant cell astrocytoma.<sup>72</sup> However, tumors are usually nonhemorrhagic and surrounded by prominent brain edema, except for metastasis. Lack of avid contrast enhancement excludes other intraventricular vascular malformations.<sup>70</sup>

Complete surgical excision is the treatment of choice for symptomatic patients with IVCMs. Conservative treatment is appropriate for asymptomatic lesions located in the supratentorial compartment. However, CMs in the third ventricle have been documented to grow rapidly and should be treated more aggressively.<sup>73,74</sup> Biopsy is not recommended due to risk of hemorrhage.

### Dural-based cavernous malformations

Dural-based CMs are rare entities that mimic meningioma. The middle cranial fossa is the most common location including the cavernous

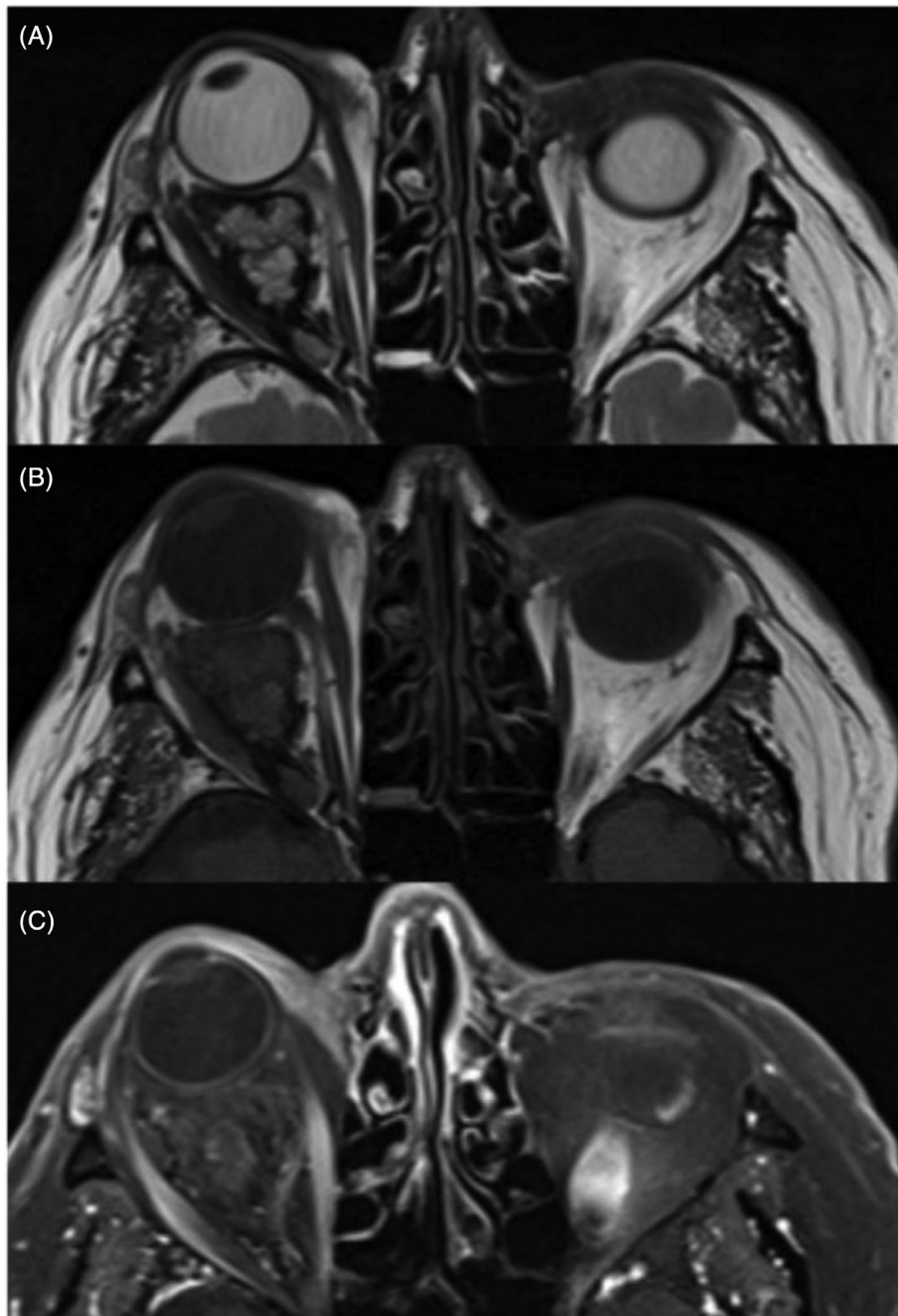


**FIGURE 17** Orbital cavernous hemangioma. Axial T2-weighted imaging (WI) (A), axial T1-WI (B), and contrast-enhanced fat-saturated T1-WI (C). Right orbital intraconal lesion with smooth contours and homogenous isointense signal on T1 and hyperintense signal on T2 and homogenous postcontrast enhancement. This is the classical appearance of an orbital cavernous hemangioma.

sinus.<sup>75</sup> They usually grow toward the middle fossa and sellar regions encasing neurovascular structures.

### Cranial nerves cavernous malformations

Isolated cranial nerves CMs are extremely rare. They can arise from almost all cranial nerves. Isolated cranial nerves CMs are extremely rare and can arise from almost all cranial nerves. CMs of the II, III, IV, V,

VI, VII/VIII, XI, and XII CN have been described.<sup>76</sup> They may be practically undetectable on imaging, except for a faint contrast enhancement, or they may mimic extra-axial tumors<sup>76</sup> (Figure 16).

### Orbital cavernous malformations conclusion

Orbital cavernous malformations (OCMs) are benign slowly progressive lesions commonly present in middle-aged adults

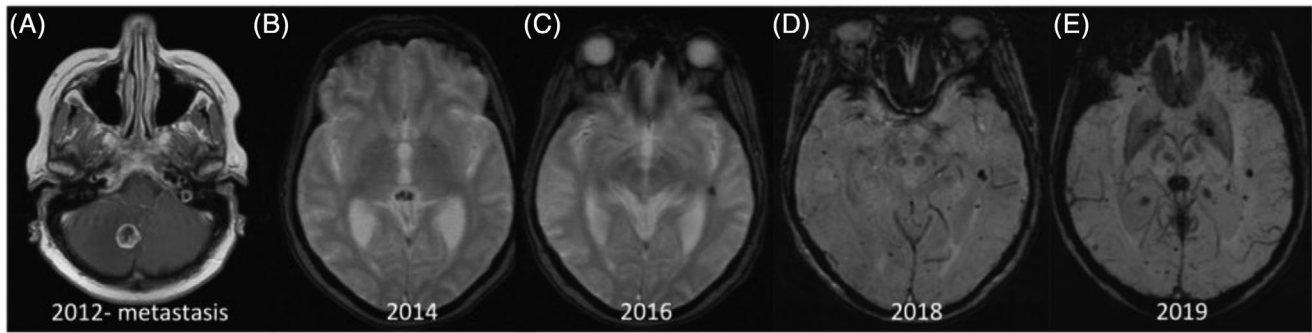


**FIGURE 18** Radiation-induced cavernous malformations. Axial contrast-enhanced T1-weighted imaging (A) of a female patient previously diagnosed with breast adenocarcinoma with a solitary central nervous system metastasis in the posterior fossa, who was later submitted to surgery and adjuvant holocranial radiotherapy. Axial gradient recalled echo (B and C) and susceptibility-weighted imaging (D and E) at 2-, 4-, 6-, and 7-years postradiotherapy, respectively. Progressive appearance of multiple discrete round parenchymal hypointense lesions, possibly representing postradiation cavernomas. However, microhemorrhages are also a typical complication of radiotherapy and can be radiologically indistinguishable

(ages 20-40 years).<sup>77</sup> CM is the most common primary benign orbital tumor in adults, constituting 6%-9% of orbital lesions.<sup>78</sup> These lesions are also known as orbital venous malformations.

OCMs are histologically like other CMs. The location and size of these lesions vary among patients. Most often, OCMs are seen as solitary intraconal lesions. Unilateral multiple lesions and bilateral lesions have been described but are extremely rare. Progressive, painless proptosis is the most common symptom. Eye movement disorders and, in rare instances, vision loss may be present.

On CT, OCMs typically present as well-circumscribed, round or ovoid, hyperattenuating intraconal lesions that displace but do not invade the adjacent structures.<sup>79</sup> On MRI, OCMs are usually isointense to muscle on T1 and hyperintense on T2 (Figure 17). After contrast administration, OCMs exhibit little and heterogeneous enhancement in early phases due to their low arterial blood flow. With passing time, contrast slowly accumulates, and enhancement gradually increases, resulting in a persistent homogeneous enhancement in the late or delayed phases of the study. This progressive “filling in” pattern is considered a pathognomonic of CM in different locations such as cavernous sinus, orbit, and liver. The main differential diagnosis includes neurofibroma, solitary fibroma, schwannoma, histiocytoma, venous varix, lymphangioma, and optic nerve sheath meningioma.<sup>78-81</sup>

Surgery should be considered if the patient has a severe visual field defect or proptosis or if new symptoms, changes, or aggravation of original symptoms occur.<sup>77,78</sup>

## RADIATION-INDUCED CAVERNOUS MALFORMATIONS

Radiation-based treatments for high-grade brain tumors may, in rare instances, induce formation of vascular malformations such as radiation-induced cavernous malformations (RICM) and capillary telangiectasias.<sup>82</sup>

It is known that RICMs take long to develop (1-35 years) after irradiation. Two pathophysiological hypotheses have been proposed. One

states that CMs may have been present before radiation, although radiographically occult, and that radiation induces growth. The second hypothesis suggests that irradiation may induce vessel wall necrosis, cell swelling, dilation of the vessel lumen, hyalinization, fibrosis, and mineralization that predispose to CM formation.<sup>83</sup>

Although the imaging appearances of RICMs are similar to those of other CMs, RICMs sometimes show mixed intensity signals with an enhancing cystic and/or solid components and an incomplete hemosiderin rim.<sup>82</sup> According to the literature, the location of these lesions after conventional whole-brain radiotherapy may be random (Figure 18).

Asymptomatic RICMs may be observed, but attention should be paid to the possibility of chronic bleeding and enlargement of the lesion. Surgical intervention should be considered in RICM cases with symptoms caused by repeated chronic hemorrhage.<sup>83</sup>

## CONCLUSION

Typical imaging characteristics of CMs have been reviewed and their diagnosis is usually straightforward. Rare locations such as extra-axial/intraventricular do not exclude the diagnosis. Multiple lesions may occur, especially in familial cases. Differentiation from tumoral pathology may not be easy as CMs may reach large dimensions and sometimes present an exuberant cystic pattern. Secondary lesions may also occur, particularly after radiation therapy. Therefore, to avoid unnecessary or inadequate further workup or treatment, the radiologist should be fully aware of the varied presentation of CMs and be able to determine whether a life-threatening situation is present that requires immediate intervention.

Follow-up strategies, including serum and imaging biomarkers, may help the management of these patients in clinical practice and prevent unnecessary surgery.

New insights in etiology have provided potential treatment options that may reduce the risk of future bleeding and/or modify the disease course. Treatment of comorbid conditions should also be



carefully considered in patients with a potentially hemorrhagic lesion.

## ACKNOWLEDGEMENTS AND DISCLOSURES

The authors declare no conflict of interest.

## ORCID

Bruno Cunha  <https://orcid.org/0000-0002-3614-2989>

Joana Ramalho  <https://orcid.org/0000-0003-4067-0589>

## REFERENCES

- Cortés Vela JJ, Concepción Aramendía L, Ballenilla Marco F, et al. Malformaciones cavernosas intracraniales: espectro de manifestaciones neurorradiológicas. *Radiología*. 2012;54:401-9.
- Patet G, Bartoli A, Meling TR. Natural history and treatment options of radiation-induced brain cavernomas: a systematic review. *Neurosurg Rev*. 2022;45:243-51.
- Rivera PP, Willinsky RA, Porter PJ. Intracranial cavernous malformations. *Neuroimaging Clin N Am*. 2003;13:27-40.
- Rotondo M, Natale M, D'Avanzo R, et al. Cavernous malformations isolated from cranial nerves: unexpected diagnosis? *Clin Neurol Neurosurg*. 2014;126:162-8.
- Abla AA, Lekovic GP, Garrett M, et al. Cavernous malformations of the brainstem presenting in childhood: surgical experience in 40 patients. *Neurosurgery*. 2010;67:1589-99.
- Del Curling O, Kelly DL, Elster AD, et al. An analysis of the natural history of cavernous angiomas. *J Neurosurg*. 1991;75:702-8.
- Son DW, Lee SW, Choi CH. Giant cavernous malformation: a case report and review of the literature. *J Korean Neurosurg Soc*. 2008;43:198.
- Robinson JR, Awad IA, Little JR. Natural history of the cavernous angioma. *J Neurosurg*. 1991;75:709-14.
- Osborn AG, Hedlund G, Salzman KL. Vascular malformations. In: Osborn AG, Hedlund G, Salzman KL, eds. *Osborn's brain*. 2nd ed. Philadelphia, PA: Elsevier; 2017:186-90.
- Dalyai RT, Ghobrial G, Awad I, et al. Management of incidental cavernous malformations: a review. *Neurosurg Focus*. 2011;31:E5.
- Ginat DT, Meyers SP. Intracranial lesions with high signal intensity on T1-weighted MR images: differential diagnosis. *Radiographics*. 2012;32:499-516.
- Deshmukh VR, Albuquerque FC, Zabramski JM, et al. Surgical management of cavernous malformations involving the cranial nerves. *Neurosurgery*. 2003;53:352-7.
- Krings T, Geibprasert S, Pereira VM, et al. Vascular malformations. In: Naidich TP, Castillo M, Cha S, et al., eds. *Imaging of the brain: expert radiology series*. Philadelphia, PA: Elsevier Health Sciences; 2012:529-67.
- Otten P, Pizzolato GP, Rilliet B, et al. 131 cases of cavernous angioma (cavernomas) of the CNS, discovered by retrospective analysis of 24,535 autopsies. *Neurochirurgie*. 1989;35:82-3, 128-31.
- Van Lindert EJ, Tan TC, Grotenhuis JA, et al. Giant cavernous hemangiomas: report of three cases. *Neurosurg Rev*. 2007;30:83-92.
- Maraire JN, Awad IA. Intracranial cavernous malformations. *Neurosurgery*. 1995;37:591-605.
- Awad IA, Polster SP. Cavernous angiomas: deconstructing a neurosurgical disease. *J Neurosurg*. 2019;131:1-13.
- Snellings DA, Hong CC, Ren AA, et al. Cerebral cavernous malformation: from mechanism to therapy. *Circ Res*. 2021;129:195-215.
- Tang AT, Choi JP, Kotzin JJ, et al. Endothelial TLR4 and the microbiome drive cerebral cavernous malformations. *Nature*. 2017;545:305-10.
- Polster SP, Sharma A, Tanes C, et al. Permissive microbiome characterizes human subjects with a neurovascular disease cavernous angioma. *Nat Commun*. 2020;11:2659.
- Tang AT, Sullivan KR, Hong CC, et al. Distinct cellular roles for PDCD10 define a gut-brain axis in cerebral cavernous malformation. *Sci Transl Med*. 2019;11:eaaw3521.
- Yun TJ, Na DG, Kwon BJ, et al. A T1 hyperintense perilesional signal aids in the differentiation of a cavernous angioma from other hemorrhagic masses. *Am J Neuroradiol*. 2008;29:494-500.
- Dorsch NWC, McMahon JHA. Intracranial cavernous malformations—natural history and management. *Crit Rev Neurosurg*. 1998;8:154-68.
- Moran NF, Fish DR, Kitchen N, et al. Supratentorial cavernous haemangiomas and epilepsy: a review of the literature and case series. *J Neurol Neurosurg Psychiatry*. 1999;66:561-8.
- Sandalcioglu IE. Surgical removal of brain stem cavernous malformations: surgical indications, technical considerations, and results. *J Neurol Neurosurg Psychiatry*. 2002;72:351-5.
- Mouchtouris N, Chalouhi N, Chitale A, et al. Management of cerebral cavernous malformations: from diagnosis to treatment. *Sci World J*. 2015;2015:1-8.
- Gross BA, Lin N, Du R, et al. The natural history of intracranial cavernous malformations. *Neurosurg Focus*. 2011;30:E24.
- Clatterbuck RE, Moriarity JL, Elmaci I, et al. Dynamic nature of cavernous malformations: a prospective magnetic resonance imaging study with volumetric analysis. *J Neurosurg*. 2000;93:981-6.
- Flemming KD, Goodman BP, Meyer FB. Successful brainstem cavernous malformation resection after repeated hemorrhages during pregnancy. *Surg Neurol*. 2003;60:545-7.
- Ojemann RG, Crowell RM, Ogilvy CS. Cranial and spinal cavernous malformations. In: Ojemann RG, Ogilvy CS, Crowell RM, et al., eds. *Surgical management of neurovascular disease*. 3rd ed. Baltimore, Md: Williams & Wilkins; 1995:538-57.
- Pozzati E, Acciarri N, Tognetti F, et al. Growth, subsequent bleeding, and de novo appearance of cerebral cavernous angiomas. *Neurosurgery*. 1996;38:662-9.
- Diogo MC, Fragata I, Pamplona J, et al. A pictorial review of the typical, atypical and the just unbelievable imaging characteristics of cavernous malformations. Presented at the European Congress of Radiology; March 4–8, 2015; Vienna.
- Zabramski JM, Wascher TM, Spetzler RF, et al. The natural history of familial cavernous malformations: results of an ongoing study. *J Neurosurg*. 1994;80:422-32.
- Abe T, Singer RJ, Marks MP, et al. Coexistence of occult vascular malformations and developmental venous anomalies in the central nervous system: MR evaluation. *AJNR Am J Neuroradiol*. 1998;19:51-7.
- Zafar A, Quadri SA, Farooqui M, et al. Familial cerebral cavernous malformations. *Stroke*. 2019;50:1294-301.
- Flemming KD, Kumar S, Lanzino G, et al. Baseline and evolutionary radiologic features in sporadic, hemorrhagic brain cavernous malformations. *Am J Neuroradiol*. 2019;40:967-72.
- Girard R, Khanna O, Shenkar R, et al. Peripheral plasma vitamin D and non-HDL cholesterol reflect the severity of cerebral cavernous malformation disease. *Biomark Med*. 2016;10:255-64.
- Girard R, Zeineddine HA, Fam MD, et al. Plasma biomarkers of inflammation reflect seizures and hemorrhagic activity of cerebral cavernous malformations. *Transl Stroke Res*. 2018;9:34-43.
- Girard R, Zeineddine HA, Koskimäki J, et al. Plasma biomarkers of inflammation and angiogenesis predict cerebral cavernous malformation symptomatic hemorrhage or lesional growth. *Circ Res*. 2018;122:1716-21.
- Akers A, Al-Shahi Salman RA, Awad I, et al. Synopsis of guidelines for the clinical management of cerebral cavernous malformations: consensus recommendations based on systematic literature review by the angioma alliance scientific advisory board clinical experts panel. *Neurosurgery*. 2017;80:665-80.



41. Morrison L, Akers A. Cerebral cavernous malformation, familial. In: Adam MP, Everman DB, Mirzaa GM, et al., eds. GeneReviews® [Internet]. Seattle, WA: University of Washington; 1993–2022.
42. Horne MA, Flemming KD, Su I-C, et al. Clinical course of untreated cerebral cavernous malformations: a meta-analysis of individual patient data. *Lancet Neurol*. 2016;15:166–73.
43. Kim BS, Kim KH, Lee MH, et al. Stereotactic radiosurgery for brainstem cavernous malformations: an updated systematic review and meta-analysis. *World Neurosurg*. 2019;130:e648–59.
44. Mespreuve M, Vanhoenacker F, Lemmerling M. Familial multiple cavernous malformation syndrome: MR features in this uncommon but silent threat. *J Belgian Soc Radiol*. 2016;100:51.
45. Shenkar R, Shi C, Rebeiz T, et al. Exceptional aggressiveness of cerebral cavernous malformation disease associated with PDCD10 mutations. *Genet Med*. 2015;17:188–96.
46. Moore SA, Brown RD, Christianson TJH, et al. Long-term natural history of incidentally discovered cavernous malformations in a single-center cohort. *J Neurosurg*. 2014;120:1188–92.
47. Chen B, Saban D, Rauscher S, et al. Modifiable cardiovascular risk factors in patients with sporadic cerebral cavernous malformations. *Stroke*. 2021;52:1259–64.
48. Brunereau L, Levy C, Laberge S, et al. De novo lesions in familial form of cerebral cavernous malformations: clinical and MR features in 29 non-Hispanic families. *Surg Neurol*. 2000;53:475–83.
49. Reitz M, Burkhardt T, Vettorazzi E, et al. Intramedullary spinal cavernoma: clinical presentation, microsurgical approach, and long-term outcome in a cohort of 48 patients. *Neurosurg Focus*. 2015;39:E19.
50. Sun I, Pamir MN. Spinal cavernomas: outcome of surgically treated 10 patients. *Front Neurol*. 2017;8:672.
51. Lawton MT, Vates GE, Quiñones-Hinojosa A, et al. Giant infiltrative cavernous malformation: clinical presentation, intervention, and genetic analysis: case report. *Neurosurgery*. 2004;55:E988–95.
52. Scott RM, Barnes P, Kupsky W, et al. Cavernous angiomas of the central nervous system in children. *J Neurosurg*. 1992;76:38–46.
53. Lobato RD, Rivas JJ, Gomez PA, et al. Comparison of the clinical presentation of symptomatic arteriovenous malformations (angiographically visualized) and occult vascular malformations. *Neurosurgery*. 1992;31:391–7.
54. Hyodo A, Yanaka K, Higuchi O, et al. Giant interdural cavernous hemangioma at the convexity. *J Neurosurg*. 2000;92:503.
55. Sansone ME, Liwnicz BH, Mandybur TI. Giant pituitary cavernous hemangioma. Case report. *J Neurosurg*. 1980;53:124–6.
56. Tokuda Y, Uozumi T, Sakoda K, et al. Giant congenital capillary hemangioma of pericranium. *Neurol Med Chir*. 1990;30:1029–33.
57. Tüzün Y, Kayaoğlu CR, Takçi E, et al. Giant cavernous hemangioma of the scalp. *Zentralbl Neurochir*. 1998;59:274–7.
58. Jhawar S, Nadkarni T, Goel A. Giant cerebral cavernous hemangiomas: a report of two cases and review of literature. *Turk Neurosurg*. 2012;22:226–32.
59. Chicani CF, Miller NR, Tamargo RJ. Giant cavernous malformation of the occipital lobe. *J Neuro-Ophthalmology*. 2003;23:151–3.
60. Hassani FD, Karekezi C, El Abbadi N. Rare case of giant pediatric cavernous angioma of the temporal lobe: a case report and review of the literature. *Surg Neurol Int*. 2020;11:7.
61. Kashiwagi S, van Loveren HR, Tew JM, et al. Diagnosis and treatment of vascular brain-stem malformations. *J Neurosurg*. 1990;72:27–34.
62. Sharma A, Mittal RS. A giant frontal cavernous malformation with review of literature. *J Neurosci Rural Pract*. 2016;07:279–82.
63. Sarwar M. Intracerebral venous angioma. *Arch Neurol*. 1978;35:323–5.
64. Scott M. Brainstem cavernous angiomas in children. *Pediatr Neurosurg*. 1990;16:281–6.
65. Bannur U, Korah I, Chandy MJ. Midbrain venous angioma with obstructive hydrocephalus. *Neurol India*. 2002;50:207–9.
66. Hasegawa T, McInerney J, Kondziolka D, et al. Long-term results after stereotactic radiosurgery for patients with cavernous malformations. *Neurosurgery*. 2002;50:1190–8.
67. Kondziolka D, Lunsford LD, Flickinger JC, et al. Reduction of hemorrhage risk after stereotactic radiosurgery for cavernous malformations. *J Neurosurg*. 1995;83:825–31.
68. Han M-S, Moon K-S, Lee K-H, et al. Cavernous hemangioma of the third ventricle: a case report and review of the literature. *World J Surg Oncol*. 2014;12:237.
69. Lee B-J, Choi C-Y, Lee C-H. Intraventricular cavernous hemangiomas located at the foramen of monro. *J Korean Neurosurg Soc*. 2012;52:144–7.
70. Kumari S, Kumar S, Kamath MT. Intraventricular cavernoma. *J Surg Surg Res*. 2018;4:001–2.
71. Katayama Y, Tsubokawa T, Maeda T, et al. Surgical management of cavernous malformations of the third ventricle. *J Neurosurg*. 1994;80:64–72.
72. Kivelev J, Niemelä M, Kivisaari R, et al. Intraventricular cerebral cavernomas: a series of 12 patients and review of the literature. *J Neurosurg*. 2010;112:140–9.
73. Reyns N, Assaker R, Louis E, et al. Intraventricular cavernomas: three cases and review of the literature. *Neurosurgery*. 1999;44:648–54.
74. Beechar VB, Srinivasan VM, Reznik OE, et al. Intraventricular cavernomas of the third ventricle: report of 2 cases and a systematic review of the literature. *World Neurosurg*. 2017;105:935–43.e3.
75. Pelluru P, Rajesh A, Uppin M. Dural-based giant cavernous hemangioma mimicking a meningioma: lessons learnt. *Neurol India*. 2017;65:1173.
76. Tavares S, Guerreiro G, Rebelo O, et al. Cavernous malformation of the III cranial nerve: a challenging pathology. *Interdiscip Neurosurg*. 2020;20:100641.
77. Harris GJ. Cavernous hemangioma of the orbital apex: pathogenetic considerations in surgical management. *Am J Ophthalmol*. 2010;150:764–73.
78. Zhang L, Li X, Tang F, et al. Diagnostic imaging methods and comparative analysis of orbital cavernous hemangioma. *Front Oncol*. 2020;10:577452.
79. Khan SN, Sepahdari AR. Orbital masses: CT and MRI of common vascular lesions, benign tumors, and malignancies. *Saudi J Ophthalmol*. 2012;26:373–83.
80. Jinhu Y, Jianping D, Xin L, et al. Dynamic enhancement features of cavernous sinus cavernous hemangiomas on conventional contrast-enhanced MR imaging. *Am J Neuroradiol*. 2008;29:577–81.
81. Wilms G, Raat H, Dom R, et al. Orbital cavernous hemangioma: findings on sequential Gd-enhanced MRI. *J Comput Assist Tomogr*. 19:548–51.
82. Guez D, Last D, Daniels D, et al. Radiation-induced vascular malformations in the brain, mimicking tumor in MRI-based treatment response assessment maps (TRAMs). *Clin Transl Radiat Oncol*. 2019;15:1–6.
83. Yu Z, Huang B, Liang R. Radiation-induced cavernous malformation after stereotactic radiosurgery for cavernous sinus meningioma: a case report. *BMC Neurol*. 2020;20:422.

**How to cite this article:** Kuroedov D, Cunha B, Pamplona J, Castillo M, Ramalho J. Cerebral cavernous malformations: Typical and atypical imaging characteristics. *J Neuroimaging*. 2022;1–16. <https://doi.org/10.1111/jon.13072>